

# An electrochemical impedance spectroscopic study of the electronic and ionic transport properties of LiCoO<sub>2</sub> cathode

ZHUANG QuanChao<sup>1,3</sup>, XU JinMei<sup>1</sup>, FAN XiaoYong<sup>1</sup>, DONG QuanFeng<sup>1,2</sup>, JIANG YanXia<sup>1</sup>, HUANG Ling<sup>1</sup> & SUN ShiGang<sup>1†</sup>

<sup>1</sup> State Key Laboratory of Physical Chemistry of Solid Surfaces, Department of Chemistry, College of Chemistry and Chemical Engineering, Xiamen University, Xiamen 361005, China;

<sup>2</sup> Power-long Battery Research Institute, Xiamen University, Xiamen 361005, China;

<sup>3</sup> Northwest Institute of Nuclear Technology, Xi'an 710024, China

**The storage behavior and process of the first delithiation-lithiation of LiCoO<sub>2</sub> cathode were investigated by electrochemical impedance spectroscopy (EIS). The electronic and ionic transport properties of LiCoO<sub>2</sub> cathode along with variation of electrode potential were obtained in 1 mol·L<sup>-1</sup> LiPF<sub>6</sub>-EC:DMC:DEC electrolyte solution. It was found that after 9 h storage of the LiCoO<sub>2</sub> cathode in electrolyte solutions, a new arc appears in the medium frequency range in Nyquist plots of EIS, which increases with increasing the storage time. In the charge/discharge processes, the diameter of the new arc is reversibly changed with electrode potential. Such variation coincides well with the electrode potential dependence of electronic conductivity of the LiCoO<sub>2</sub>. Thus this new EIS feature is attributed to the change of electronic conductivity of Li<sub>x</sub>CoO<sub>2</sub> during storage of the LiCoO<sub>2</sub> cathode in electrolyte solutions, as well as in processes of intercalation-deintercalation of lithium ions. It has been revealed that the reversible increase and decrease of the resistance of SEI film in charge-discharge processes can be also ascribed to the variation of electronic conductance of active materials of the LiCoO<sub>2</sub> cathode.**

Li-ion batteries, LiCoO<sub>2</sub>, EIS, SEI film, electronic conductivity

LiCoO<sub>2</sub> is the most widely used cathode material today in commercially available Li-ion batteries, due to its high energy density, low self-discharge and good cycle life performance<sup>[1–3]</sup>. In the past decade, the LiCoO<sub>2</sub> and, in general, its derivatives Li<sub>x</sub>Ni<sub>1-y</sub>Co<sub>y</sub>O<sub>2</sub> have been studied extensively as cathode materials for Li-ion batteries. However, the electronic conductivity, electronic structure, and phase transitions of these cathode materials as well as the effect of these properties on electrochemical performance need to be investigated in detail<sup>[4–7]</sup>. The literature data<sup>[2,8–10]</sup> leave no doubts about the existence of a drastic change of the electronic conductivity occurring at early stage of lithium deintercalation, which may be caused by a transition from insulator to metal (or so called metal-insulator transition). In case of Li<sub>x</sub>CoO<sub>2</sub>

materials, such transition has been proposed to be responsible for the existence of a two-phase region between the lithium concentrations of  $x = 0.95$  and  $x = 0.75$ , namely, Li<sub>x</sub>CoO<sub>2</sub> is a semiconductor for  $x > 0.95$ , and is of metallic property for  $x < 0.75$ .

Electrochemical impedance spectroscopy (EIS), is one of the most powerful means to analyze electrochemical processes occurring at electrode/electrolyte interfaces, and has been widely applied to the studies of electrochemical lithium intercalation into carbonaceous materials and transition metal oxides. The Nyquist plots

Received September 7, 2006; accepted December 28, 2006  
doi: 10.1007/s11434-007-0169-1

†Corresponding author (email: sgsun@xmu.edu.cn)

Supported by the Special Funds for Major State Basic Research Project of China (Grant No. 2002CB211804)

of electrochemical lithium intercalation into  $\text{LiCoO}_2$ -based electrodes commonly consist of three parts, namely, the first arc in the high-frequency range (HFA), the second arc in the medium frequency (MFA) range, and an incline line in the low frequency range. The HFA is generally attributed to the migration of lithium ions through a surface film (also called solid electrolyte interphase (SEI)) on  $\text{LiCoO}_2$ , the MFA is ascribed to the charge transfer step, and the incline line in the low frequency range reflects the solid state diffusion process of lithium ions into  $\text{LiCoO}_2$  that is often described as finite space or restricted diffusion<sup>[11–15]</sup>. However, Croce and coworkers<sup>[16–21]</sup> considered that the drastic change in resistance caused by the insulator to metal transition must be necessarily reflected by the impedance dispersion, namely, the Nyquist plots of  $\text{LiCoO}_2$  in the delithiated state should involve a third arc relating to the electronic properties of the material. Therefore, the Nyquist plots of electrochemical lithium intercalation into  $\text{LiCoO}_2$ -based electrode should include four parts, i.e. the first arc in the high-frequency range (HFA), the second arc in the medium-frequency range (MFA), the third arc in the low-frequency range (LFA), and an incline line in the very low frequency range. They proposed that the HFA is related to the migration of lithium ions through SEI film on the  $\text{LiCoO}_2$  electrode, the MFA is attributed to the charge transfer step, the LFA is associated with the electronic properties of the material, and the incline line in the very low frequency range reflects the ionic diffusion. The experimental results of Croce et al. were nevertheless analogous to those previously reported by other authors, and from their Nyquist plots, the three obviously separated semicircles could not be observed. Moreover, the Nyquist plots of electrodes of the  $\text{LiCoO}_2$  and its derivative materials  $\text{Li}_x\text{Ni}_{1-y}\text{Co}_y\text{O}_2$ , which they obtained at low potentials (below 3.7 V), were also analogous to previously reported results consisting of two parts: 1) an arc in the high-frequency range relating to migration of lithium ions through the SEI film, and 2) a sloping line in the low-frequency range that is generally attributed to the charge transfer process or the blocking characteristic of the electrode. Croce and coworkers<sup>[16–21]</sup> attributed nevertheless the sloping line in low-frequency range to the electronic properties of the material. It is well known that the practical  $\text{LiCoO}_2$  cathodes are composite materials, in which the active mass particles are bound to an aluminum current

collector with a polymeric binder such as polyvinylidene difluoride (PVdF). In addition, the composite electrodes have to contain a conductive additive, usually carbon particles (e.g. carbon black, graphite). The electrodes are usually prepared from slurry of the particles and the binder in an organic solvent, which is spread on the current collector, followed by drying. The final shape of the electrode is obtained by applying some pressure to the electrode. So, its electronic conductivity must be affected by the amount of conductive additive in the  $\text{LiCoO}_2$  composite materials and by the contact between the  $\text{LiCoO}_2$  cathode film and the aluminum current collector. As a consequence, variation of electronic conductivity of the active mass with electrode potential change can be observed only when the  $\text{LiCoO}_2$  cathode contains enough amount of conductive additive, and has a good contact between the  $\text{LiCoO}_2$  cathode film and the aluminum current collector. In addition, when the  $\text{LiCoO}_2$  cathode contacts non-aqueous organic electrolytes, spontaneous reactions may take place at surface of the cathode and form a thick surface film on it. Along with the dissolution of lithium ions from  $\text{LiCoO}_2$  electrochemical inactive  $\text{Co}_3\text{O}_4$  may be formed<sup>[22–24]</sup>. It can be deduced that the electronic conductivity of the  $\text{LiCoO}_2$  cathode may be greatly affected by the above processes. Based on the above analysis, the  $\text{LiCoO}_2$  cathode containing high weight percent of conductive additive and PVdF binder (10 wt%) was prepared in this study, and the  $\text{LiCoO}_2$  cathode after drying was compressed by a rolling machine (between iron wheels) in order to obtain a good contact between the  $\text{LiCoO}_2$  cathode film and the aluminum current collector. The storage behavior and process of first delithiation-lithiation of the  $\text{LiCoO}_2$  cathode were investigated by EIS. The electronic and ionic transport properties of the  $\text{LiCoO}_2$  cathode were obtained for the storage and the process of the first delithiation-lithiation in  $1 \text{ mol}\cdot\text{L}^{-1}$   $\text{LiPF}_6\text{-EC}\cdot\text{DMC}\cdot\text{DEC}$  electrolyte solutions.

## 1 Experiment

All experiments were carried out in a three-electrode glass cell with Li foils as both auxiliary and reference electrodes. The  $\text{LiCoO}_2$  cathode composition was 80 weight percent (wt%)  $\text{LiCoO}_2$  powder (B&M Ltd Co., Tianjin, China), 10 wt% polyvinylidene fluoride binder (Kynar FLEX 2801, Elf-atochem, USA), 3 wt% carbon black and 7 wt% graphite (Shanshan limited Co.

Shanghai, China), and an aluminum foil was used as current collector. The electrolyte was 1 mol·L<sup>-1</sup> LiPF<sub>6</sub>-EC:DMC:DEC (volume ratio 1:1:1, Guotaihuarong Co., Zhangjiagang, China).

EIS measurements were carried out in an electrochemical work station (CHI660b, Chenhua Ltd Co., Shanghai, China). The amplitude of ac perturbation signal was 5 mV and the frequency range was from 10<sup>5</sup> to 10<sup>-2</sup> Hz. The electrode was equilibrated for 1 h before EIS measurements. The impedance data were analyzed using Zview software.

## 2 Results and discussion

### 2.1 The common EIS features of LiCoO<sub>2</sub> cathode in the storage and in the first charge-discharge process

The Nyquist plots (Figure 1(a)) for the storage of LiCoO<sub>2</sub> cathode for 3 and 6 h in electrolyte solutions at open circuit potential, i.e. 3.5 V, display an arc in the high-frequency (HF) range and a slightly inclined line in the low-frequency (LF) region, similar to the results reported in refs. [11–21]. As previously described, the arc in the high-frequency range is related to the migration of lithium ions through SEI film, and the sloping line in the low-frequency range is generally attributed to the charge transfer process or the blocking characteristic of the electrode<sup>[11–15]</sup>. However, Croce and coworkers attributed the sloping line in the low-frequency range to electronic properties of the material<sup>[16–21]</sup>.

It is found that after 9 h storage of the LiCoO<sub>2</sub> cathode in electrolyte solutions, a new arc appears in the medium frequency range (MFA) in Nyquist plots. This new arc increases with the increase of the storage time,

but the EIS features remain unchanged till 42 h of storage (Figure 1(b)). The above unique phenomenon has not been reported so far in the literature to our knowledge. Because the electrode potential was set at 3.5 V in the storage of LiCoO<sub>2</sub> cathode in electrolyte solutions, the appearance of the new arc must associate with the interaction between LiCoO<sub>2</sub> cathode and electrolyte solution species. This corresponds to our previous analysis that in the storage of LiCoO<sub>2</sub> cathode in electrolyte solution, spontaneous reactions may take place at surface of the cathode resulting in a thick surface film, and the dissolution of lithium ions from LiCoO<sub>2</sub> leads to the formation of electrochemically inactive Co<sub>3</sub>O<sub>4</sub>. The above processes give rise to change of the electronic conductivity of LiCoO<sub>2</sub>. Obviously, if the new arc is attributed to charge transfer step according to Croce et al., the above phenomenon could not be explained properly. Thus the new arc appearing in the medium frequency range in the Nyquist plots after 9 h storage of LiCoO<sub>2</sub> cathode in electrolyte solutions should be assigned to electronic properties of the material, and the HFA, MFA, LFA appearing in the Nyquist plots in Figure 1(b) may be attributed to the migration of lithium ions through the SEI films, the electronic properties of the material and the charge transfer step, respectively.

Variations of impedance spectra of LiCoO<sub>2</sub> cathode after 42 h storage in electrolyte solution with increase of polarization potential (charge process) are shown in Figure 2. It can be seen that along with increase of electrode potential, the EIS features of LiCoO<sub>2</sub> cathode below 3.85 V in the charge process are analogous to those obtained after 9 h storage in electrolyte solution. On charging from 3.85 to 3.9 V, the diameter of the MFA

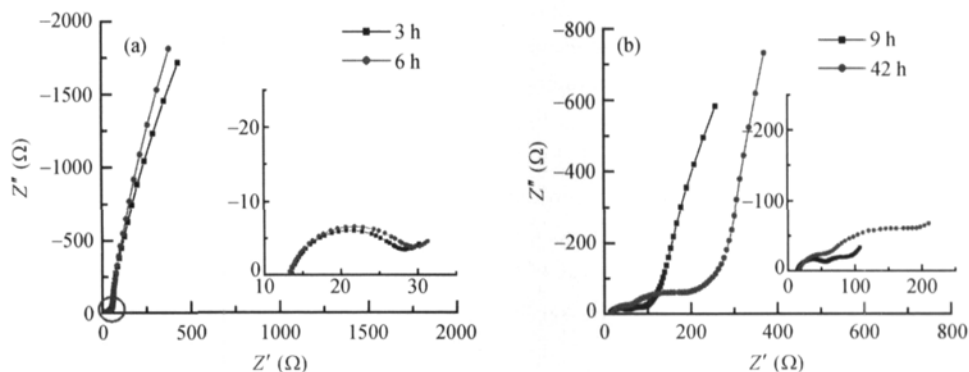


**Figure 1** Variations of impedance spectra of LiCoO<sub>2</sub> cathode with the increase of the storage time in frequency range 10<sup>5</sup>–10<sup>-2</sup> Hz. The insets in (a) and (b) show the enlarged spectra over a 10<sup>5</sup>–50 Hz and 10<sup>5</sup>–0.5 Hz frequency range respectively.

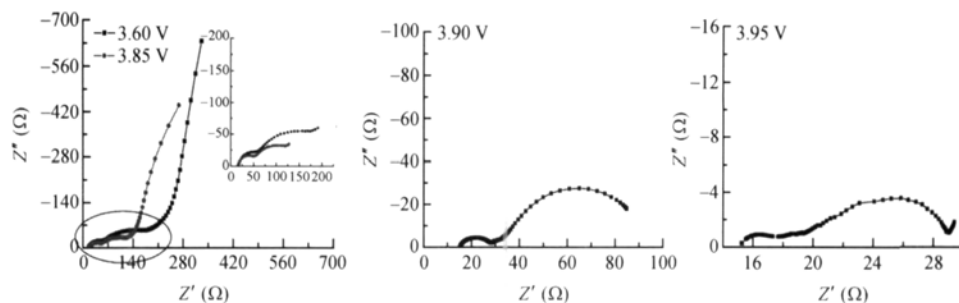


**Figure 2** Variations of impedance spectra of LiCoO<sub>2</sub> cathode after 42 h storage in the electrolyte solution with the polarization potential in the first charge process in frequency range 10<sup>5</sup>–10<sup>2</sup> Hz. The inset shows the enlarged spectra over a 10<sup>5</sup>–0.5 Hz frequency range.

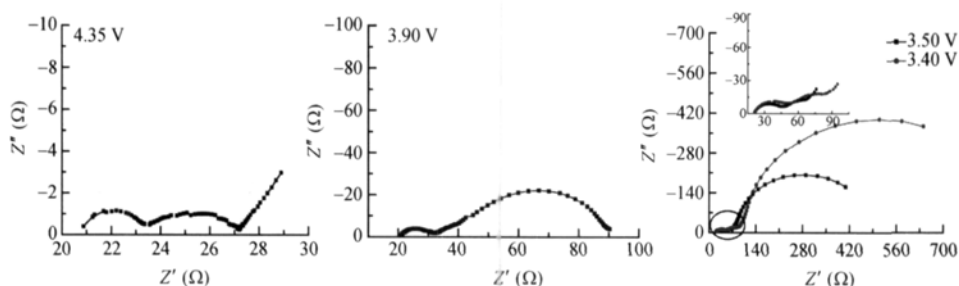


**Figure 3** Variations of impedance spectra of LiCoO<sub>2</sub> cathode with the polarization potential in the first discharge process in frequency range 10<sup>5</sup>–10<sup>2</sup> Hz. The inset shows the enlarged spectra over a 10<sup>5</sup>–1 Hz frequency range.

decreases rapidly. We could not observe clearly a semicircle in the medium frequency range, the MFA is converted into a sloping line due to the large diameter of the HFA, and the inclined line related to charge transfer step in the low frequency range is bended toward the real axis forming a semicircle. At 3.95 V, a straight line reflecting the solid state diffusion of lithium ions into LiCoO<sub>2</sub> appears in the very low frequency range in the Nyquist plots. Thus the spectrum at 3.95 V yields an HFA related to SEI film, a second arc in the medium-frequency region associated with electronic conductivity of the LiCoO<sub>2</sub>, and a third arc in the low-frequency range corresponding to charge transfer resistance coupled with double layer capacitance, followed by a straight line reflecting solid state Li-ion diffusion in the bulk of active mass in the very low frequency range. On further charging to 4.35 V, the EIS features of LiCoO<sub>2</sub> cathode remain analogous to those at 3.95 V in the charge process.

Figure 3 shows variations of impedance spectra of LiCoO<sub>2</sub> cathode with the decrease of electrode potential (discharge process). In the experiment, the electrode

potential was first swept linearly to 4.35 V at 20 μV/s, and then impedance spectra were recorded along with the decrease of electrode potential. We could not observe three well-separated semicircles at 4.35 V in Nyquist plots due to overlapping of the HFA and the MFA when their diameters are too small. With the decrease of electrode potential, the EIS features of the LiCoO<sub>2</sub> cathode above 3.95 V are similar to those at 4.35 V; the EIS features of the LiCoO<sub>2</sub> cathode at 3.9 V in discharge process are analogous to those observed at 3.9 V in charge process; a sloping line appears in the medium frequency range and the straight line in the very low frequency range disappears. On further discharging to 3.4 V, the sloping line is converted to a semicircle, while the LFA is translated to a sloping line.

## 2.2 Equivalent circuit proposed in EIS analysis

According to experimental results obtained in this work, an equivalent circuit, as shown in Figure 4, is proposed to fit the impedance spectra in the storage and the first charge-discharge process. In this equivalent circuit,  $R_s$  represents the ohmic resistance;  $R_{SEI}$  and  $R_{ct}$  are resistances of the SEI film and the charge transfer reaction;

the capacitance of the SEI film, the capacitance of the double layer and the Warburg impedance are represented by the constant phase elements (CPE)  $Q_{\text{SEI}}$ ,  $Q_{\text{dl}}$  and  $Q_{\text{D}}$ , respectively; the electronic resistance of the material and the associated capacitance used to characterize the electronic properties of the material are represented by  $R_{\text{e}}$  and the constant phase elements  $Q_{\text{e}}$ . The expression for the admittance response of the CPE ( $Q$ ) is

$$Y = Y_0 \omega^n \cos\left(\frac{n\pi}{2}\right) + j Y_0 \omega^n \sin\left(\frac{n\pi}{2}\right), \quad (1)$$

where  $\omega$  is the angular frequency,  $j$  the imaginary unit. A CPE represents a resistor when  $n = 0$ , a capacitor with capacitance of  $C$  when  $n = 1$ , an inductor when  $n = -1$ , and a Warburg resistance when  $n = 0.5$ . In this study,  $Y_0$  is considered to be a pseudo capacitance (pseudo- $Y_0$ ) when  $n$  lies between 0.5 and 1.

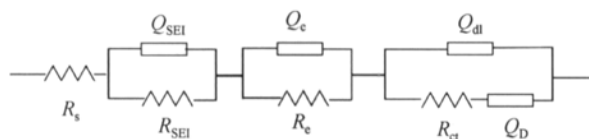


**Figure 4** Equivalent circuit proposed for analysis of impedance spectra of LiCoO<sub>2</sub> cathode in the storage in electrolyte and the first charge-discharge process.

The simulated impedance spectra are compared with experimental EIS data at 3.5 V in the discharge process in Figure 5, and the parameter values are listed in Table 1. It can be seen that the proposed model can satisfactorily describe the experimental data. The relative standard deviation for all parameters fitted does not exceed 15%.

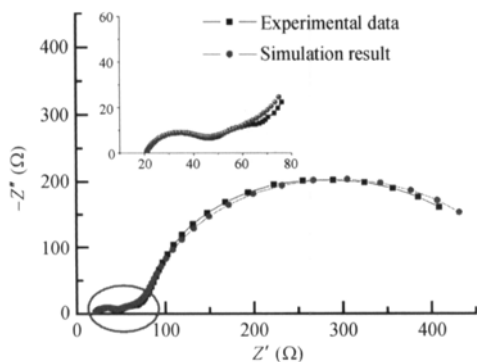


**Figure 5** Comparison of EIS experimental data at 3.5 V in the discharge process with simulation results using equivalent circuit of Figure 4.

### 2.3 Storage behavior of the LiCoO<sub>2</sub> cathode in electrolyte solutions

Figure 6 shows variations of EIS parameters obtained from fitting the experimental impedance spectra of the LiCoO<sub>2</sub> cathode with increasing the storage time at open circuit potential. It can be seen that with the increase of storage time,  $R_{\text{SEI}}$  and  $Q_{\text{SEI}-n}$  keep invariable, while  $Q_{\text{SEI}-Y_0}$  continuously increases till 30 h storage, and keeps invariable after 30 h storage. These results indicate that a highly passivating SEI film has been formed on surface of the LiCoO<sub>2</sub> cathode after 9 h storage, thus the aging process of the SEI film dominates the electrode surface chemistry between 9 and 30 h. It is well known that the electrolyte solutions may be unavoidably contaminated by trace water, and in the aging process of the SEI film H<sub>2</sub>O may react with components of the SEI film such as organic carbonate lithium compounds ROCO<sub>2</sub>Li to yield Li<sub>2</sub>CO<sub>3</sub>, leading to the dissolution of part of organic components of the SEI film and to the increase of capacitance of the SEI film.

**Table 1** Equivalent circuit parameters obtained from simulation of EIS experimental data at 3.5 V in the discharge process

Parameter	Value	Uncertainty
$R_s$ ( $\Omega$ )	20.75	0.70549%
$R_{\text{SEI}}$ ( $\Omega$ )	24.47	4.085%
$Q_{\text{SEI}-Y_0}$ (F)	$3.4614 \times 10^{-5}$	15.903%
$Q_{\text{SEI}-n}$	0.77337	2.2416%
$R_e$ ( $\Omega$ )	29.66	7.6092%
$Q_e-Y_0$ (F)	0.002062	13.736%
$Q_e-n$	0.69975	5.9917%
$R_{\text{ct}}$ ( $\Omega$ )	465.2	1.775%
$Q_{\text{dl}}-Y_0$ (F)	0.0084102	1.3786%
$Q_{\text{dl}}-n$	0.91124	0.94703%
$\chi^2=0.0012681$		

With the increase of storage time,  $R_{\text{e}}$  increases,  $Q_{\text{e}-n}$  keeps invariable, while  $Q_{\text{e}-Y_0}$  decreases, implying that the electronic conductivity of the material is strongly affected by the storage time of the LiCoO<sub>2</sub> cathode in electrolyte solutions. Because the electrode potential is always maintained at 3.5 V during storage of the LiCoO<sub>2</sub> cathode in electrolyte solution, we may conclude that the electronic conductivity is affected not solely by the electrode potential, but the storage time of the LiCoO<sub>2</sub> cathode in electrolyte solutions plays a major role. Wang et al. reported that the storage of LiCoO<sub>2</sub> in electrolyte solutions may lead to the dissolution of lithium ions from LiCoO<sub>2</sub> and the formation of electrochemically inactive Co<sub>3</sub>O<sub>4</sub> compound. Therefore the variation of electronic

conductivity in storage of the LiCoO<sub>2</sub> cathode in electrolyte solutions may be ascribed to the degradation in structure of the LiCoO<sub>2</sub>.

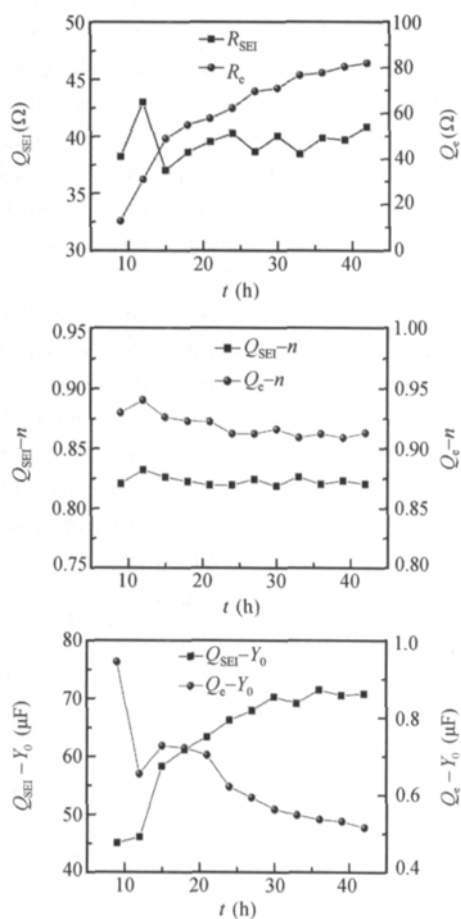


**Figure 6** Variations of EIS parameters obtained from fitting the experimental impedance spectra of the LiCoO<sub>2</sub> cathode with the increase of storage time at open circuit potential (OCP, 3.5 V).

#### 2.4 EIS studies of the LiCoO<sub>2</sub> cathode in the first charge-discharge process

Variations of  $R_{SEI}$  and  $R_c$  with increase and decrease of electrode potential obtained from fitting the experimental impedance spectra of the LiCoO<sub>2</sub> cathode in the first charge-discharge process are shown in Figures 7 and 8, respectively. It can be observed that with the increase of electrode potential in the charge process,  $R_{SEI}$  decreases slowly below 3.8 V, decreases rapidly between 3.8 and 3.95 V, and decreases slowly again at more positive potentials, and along with decrease of electrode potential in the discharge process,  $R_{SEI}$  increases slowly above 4.0 V, and increases rapidly below 4.0 V. The results demonstrate that the resistance of the SEI film increases and

decreases reversibly in the charge-discharge process. There are two possibilities that may lead to the reversible change in  $R_{SEI}$ : 1) the resistive SEI film is reversibly breakdown (or dissolution); and 2) the variation in surface electronic conductance of the LiCoO<sub>2</sub> cathode is caused by a phase transition of delithiation-lithiation. It can be seen from Figures 7 and 8 that the increase or decrease of  $R_{SEI}$  is always concomitant with the increase or decrease of  $R_c$  in the charge-discharge process, thus the reversible change of the  $R_{SEI}$  in charge-discharge process should be ascribed to the variation in surface electronic conductance of the LiCoO<sub>2</sub> cathode.

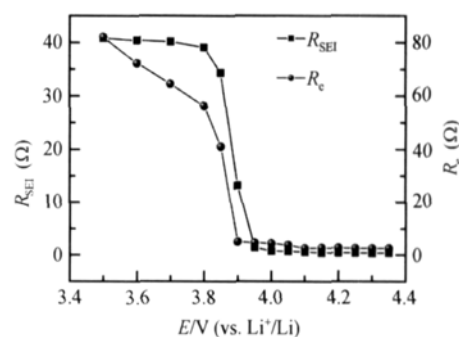


**Figure 7** Variations of  $R_{SEI}$  and  $R_c$  with the increase of the electrode potential obtained from fitting the experimental impedance spectra of the LiCoO<sub>2</sub> cathode in the first charge process.

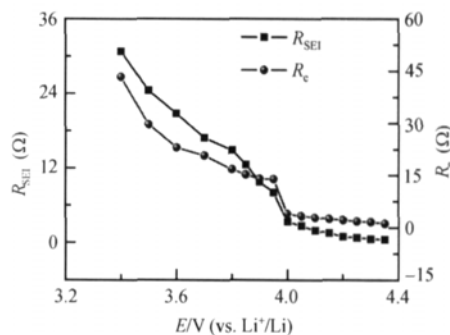


**Figure 8** Variations of  $R_{SEI}$  and  $R_c$  with the decrease of the electrode potential obtained from fitting the experimental impedance spectra of the LiCoO<sub>2</sub> cathode in the first discharge process.

When electrode potential is increasing in the charge process,  $R_c$  decreases rapidly below 3.9 V, and remains almost invariable above 3.9 V. However, with the decrease of electrode potential in the discharge process,  $R_c$  keeps almost invariable above 4.0 V and increases rapidly below 4.0 V. These experimental results are in accordance with those reported by Shibubuya et al.<sup>[4]</sup>, i.e. the electronic conductivity of LiCoO<sub>2</sub> increases expo-

nentially with electrode potential in the region from 3.0 to 3.9 V, and the electronic conductivity is saturated above 3.9 V. The potential-conductivity profile shows reasonable reversibility when the potential scan is reversed at 4.0 V. Moreover,  $R_e$  is 82  $\Omega$  at 3.5 V in the charge process, which is between 2.5 and 5  $\Omega$  above 3.9 V, being also in accordance with the results reported by Shibuya et al. that the electronic conductivity of  $\text{LiCoO}_2$  increases by one or two orders of magnitude.

The above results and discussions demonstrated that assigning the MFA in Nyquist plots of the  $\text{LiCoO}_2$  cathode to electronic conductive properties of the material could explain the drastic change of the electronic conductivity occurring at the early stage of lithium deintercalation, which has further confirmed our hypothesis and analysis.

## 2.5 Discussion on the electronic properties of $\text{LiCoO}_2$

It is well known that<sup>[25-27]</sup>  $\text{LiCoO}_2$  is a p-type semiconductor (band-gap  $E_g = 2.7$  eV), while  $\text{Li}_x\text{CoO}_2$  exhibits a metal-like behavior for  $x < 0.75$ .  $\text{Li}_x\text{CoO}_2$  is predicted to have partially filled valence bands for  $x$  lower than 1.0. For each Li removed from  $\text{LiCoO}_2$  lattice, an electron hole is created within the valence band, namely,

$$p = 1 - x, \quad (2)$$

where  $p$  is the concentration of electron hole. We may expect that there will be sufficient holes, when  $x$  is below 0.75, to allow for a significant degree of screening. And in this regime, the hole state in the valence bands is likely to be delocalized, so that  $\text{Li}_x\text{CoO}_2$  exhibits metallic-like electronic properties. This behavior is clearly observed in infrared absorption spectra where a strong absorption by holes occurs at low wave-numbers<sup>[25]</sup>. Accordingly, the variation with potential of electronic conductivity of  $\text{LiCoO}_2$  in the charge-discharge process may be divided into three regions: 1) the region in which  $\text{Li}_x\text{CoO}_2$  has a semiconductor-like behavior; 2) the region in which the hole state in the valence bands is likely to be delocalized; 3) the region in which  $\text{Li}_x\text{CoO}_2$  has a metal-like behavior.

The general expression for the electronic conductivity for p-type semiconductor is given by eq. (3).

$$\sigma = pq\mu, \quad (3)$$

where  $\mu$  is carrier hole mobility, and  $q$  is electron charge.

The electronic resistance  $R$  can be written as

$$R = \frac{S}{\sigma l}, \quad (4)$$

where  $l$  is the thickness of the material, and  $S$  is the material's area.

The Langmuir insertion isotherm could be used for lithium-ion deintercalation from  $\text{LiCoO}_2$  hosts by assuming that the interaction between the intercalated species and the host material and the interaction between the intercalated species are absent. Thus, the intercalation level,  $x$ , is given by<sup>[28]</sup>

$$x/(1-x) = \exp[f(E - E_0)], \quad (5)$$

where  $f = F/RT$  ( $F$  and  $R$ , Faraday and gas constant respectively;  $T$ , absolute temperature),  $E$  and  $E_0$  define the electrode's real and standard potentials in the equilibrium.

When eq. (2) is introduced into eq. (5), the concentration of electron holes is given by

$$p = 1 / \{1 + \exp[f(E - E_0)]\}. \quad (6)$$

Thus it can be obtained from eqs. (3), (4) and (6):

$$\ln R = \ln(S/q\mu l) + \ln\{1 + \exp[f(E - E_0)]\}. \quad (7)$$

When  $\exp[f(E - E_0)]$  is small, as in the present case,  $\ln\{1 + \exp[f(E - E_0)]\}$  could be linearized by using Taylor series expansion. As a consequence, eq. (7) can be written as

$$\ln R = \ln(2S/q\mu l) + \frac{1}{2}f(E - E_0). \quad (8)$$

It can be seen from Figure 8 that the value of  $\ln R$  shows a linear dependence on electrode potential. Therefore, the variation of the electronic conductivity of  $\text{LiCoO}_2$  in charge-discharge process with potential may be divided into three different parts: 1) when  $\text{Li}_x\text{CoO}_2$  has a semiconductor-like behavior, the value of  $\ln R_e$  shows a linear dependence on electrode potential; 2) when the hole state in the valence bands is likely to be delocalized, the value of  $\ln R_e$  increases or decreases drastically with electrode potential; 3) when  $\text{Li}_x\text{CoO}_2$  has a metal-like behavior, the value of  $\ln R_e$  also exhibits a linear dependence on electrode potential.

Figure 9 displays the variations of the logarithm of  $R_e$  of  $\text{LiCoO}_2$  with electrode potential. It can be observed that the experimental values of  $\ln R_e$  show a linear dependence on electrode potential below 3.85 V and above 3.9 V, increasing drastically between 3.85 and 3.9 V in

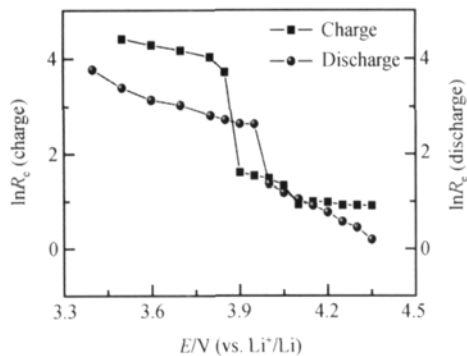


**Figure 9** Variations of the logarithm of  $R_e$  with the increase and decrease of the electrode potential.

the charge process. However, the linear dependence of the experimental values of  $\ln R_e$  on electrode potential is distorted, probably due to the complicated surface phenomena taking place in the first charge process. The experimental values of  $\ln R_e$  below 3.95 V and above 4.0 V all show a good linear dependence on electrode potential and the  $\ln R_e$  increases drastically between 3.95 and 4.0 V in the discharge process. The above results indicate that the dependence of the experimental values of  $\ln R_e$  on electrode potential is in accord with theoretical prediction, which further confirms that the MFA in the

Nyquist plots should be attributed to the electronic properties of  $\text{LiCoO}_2$  caused by delithiation.

### 3 Conclusions

The storage behavior and the first delithiation-lithiation process of  $\text{LiCoO}_2$  cathode were investigated by electrochemical impedance spectroscopy. The electronic and ionic transport properties of the  $\text{LiCoO}_2$  cathode with variation of electrode potential were obtained in  $1 \text{ mol}\cdot\text{L}^{-1}$   $\text{LiPF}_6\text{-EC:DMC:DEC}$  electrolyte solution. It was found that after 9 h storage of the  $\text{LiCoO}_2$  cathode in the electrolyte solution, a new arc appears in the medium frequency range in Nyquist plots. This new arc increases with increase of the storage time. Moreover, the new arc reversibly increases and decreases with the variation of electrode potential. Such phenomenon corresponds to the variation of electronic conductivity of the  $\text{LiCoO}_2$  with potential, and the new arc has been ascribed consequently to electronic properties of the  $\text{LiCoO}_2$  cathode. It has also been revealed that the reversible increase and decrease of the resistance of SEI film in the charge- discharge process might be ascribed to the variation of the surface electronic conductance of the  $\text{LiCoO}_2$  cathode.

- Johnson B A, White R E. Characterization commercially available lithium-ion batteries. *J Power Sources*, 1998, 70: 48–54
- Antolini E.  $\text{LiCoO}_2$ : formation, structure, lithium and oxygen non-stoichiometry, electrochemical behaviour and transport properties. *Solid State Ionics*, 2004, 170: 159–171
- Chen Z, Dahn J R. Methods to obtain excellent capacity retention in  $\text{LiCoO}_2$  cycled to 4.5 V. *Electrochimica Acta*, 2004, 49: 1079–1090
- Shibubuya M, Nishina T, Matsue T, et al. *In situ* conductivity measurements of  $\text{LiCoO}_2$  film during insertion/extraction by using interdigitated microarray electrodes. *J Electrochem Soc*, 1996, 143: 3157–3160
- Tukamoto H, West A R. Electronic conductivity of  $\text{LiCoO}_2$  and its enhancement by magnesium doping. *J Electrochem Soc*, 1997, 144: 3164–3168.
- Lala S M, Montoro L A, Lemos V, et al. The negative and positive structural effects of Ga doping in the electrochemical performance of  $\text{LiCoO}_2$ . *Electrochimica Acta*, 2005, 51: 7–13
- Cao H, Xia B, Zhang Y, et al.  $\text{LiAlO}_2$ -coated  $\text{LiCoO}_2$  as cathode material for lithium ion batteries. *Solid State Ionics*, 2005, 176: 911–914
- Ceder G, Van der Ven A. Phase diagrams of lithium transition metal oxides: investigations from first principles. *Electrochimica Acta*, 1999, 45: 131–150
- Van der Ven A, Aydinol M K, Ceder G, et al. First-principles investigation of phase stability in  $\text{Li}_x\text{CoO}_2$ . *Phys Review B*, 1998, 58(6): 2975–2987
- van Elp J, Wieland J L, Eskes H, et al. Electronic structure of  $\text{CoO}$ ,  $\text{Li-doped CoO}$  and  $\text{LiCoO}_2$ . *Phys Review B*, 1991, 44(12): 6090–6103
- Thomas M G S R, Bruce P G, Goodenough J B. AC impedance analysis of polycrystalline insertion electrodes: Application to  $\text{Li}_{1-x}\text{CoO}_2$ . *J Electrochem Soc*, 1985, 132(7): 1521–1528
- Gnanaraj J S, Cohen Y S, Levi M D, et al. The effect of pressure on the electroanalytical response of graphite anodes and  $\text{LiCoO}_2$  cathodes for Li-ion batteries. *J Electroanal Chem*, 2001, 516: 89–102
- Levi M D, Gamolsky K, Aurbach D, et al. On electrochemical impedance measurements of  $\text{Li}_x\text{Co}_{0.2}\text{Ni}_{0.8}\text{O}_2$  and  $\text{Li}_x\text{NiO}_2$  intercalation electrodes. *Electrochimica Acta*, 2000, 45: 1781–1789
- Aurbach D, Markovsky B, Levi M D, et al. New insights into the interactions between electrode materials and electrolyte solutions for advanced nonaqueous batteries. *J Power Sources*, 1999, 81-82: 95–111
- Levi M D, Salitra G, Markovsky B, et al. Solid-state electrochemical kinetics of Li-ion intercalation into  $\text{Li}_{1-x}\text{CoO}_2$ : simultaneous application of electroanalytical techniques SSCV, PITT, and EIS. *J Elec-*

- trochem Soc, 1999, 146: 1279–1289
- 16 Nobili F, Dsoke S, Corce F, et al. An ac impedance spectroscopy study of Mg-doped LiCoO<sub>2</sub> at different temperatures: electronic and ionic transport properties. *Electrochimica Acta*, 2005, 50: 2307–2313
  - 17 Nobili F, Tossici R, Croce F, et al. An electrochemical ac impedance study of Li<sub>x</sub>Ni<sub>0.75</sub>Co<sub>0.25</sub>O<sub>2</sub> intercalation electrode. *J Power Sources*, 2001, 94: 238–241
  - 18 Nobili F, Tossici R, Marassi R, et al. An ac impedance study of Li<sub>x</sub>-CoO<sub>2</sub> at different temperatures. *J Phys Chem B*, 2002, 106: 3909–3915
  - 19 Croce F, Nobili F, Deptula A, et al. An electrochemical impedance study of the transport properties of LiNi<sub>0.75</sub>Co<sub>0.25</sub>O<sub>2</sub>. *Electrochem Commun*, 1999, 1: 605–608
  - 20 Nobili F, Croce F, Scrosati B, et al. Electronic and electrochemical properties of Li<sub>x</sub>Ni<sub>1-x</sub>CoO<sub>2</sub> cathodes studied by impedance spectroscopy. *Chem Mater*, 2001, 13: 1642–1646
  - 21 Nobili F, Dsoke S, Minicucci M, et al. Correlation of ac-impedance and *in-situ* X-ray spectra of LiCoO<sub>2</sub>. *J Phys Chem B*, 2006, 110(23): 11310–11313
  - 22 Wang Z, Huang X, Chen L. Characterization of spontaneous reactions of LiCoO<sub>2</sub> with electrolyte solvent for lithium-ion batteries. *J Electrochem Soc*, 2004, 151: A1641–A1652
  - 23 Wang Z, Chen L. Solvent storage-induced structural degradation of LiCoO<sub>2</sub> for lithium ion batteries. *J Power Sources*, 2005, 146: 254–258
  - 24 Liu N, Li H, Wang Z, et al. Origin of solid electrolyte interphase on nanosized LiCoO<sub>2</sub>. *Electrochem Solid-State Lett*, 2006, 9(7): A328–A331
  - 25 Julien C M. Lithium intercalated compounds charge transfer and related properties. *Materials Sci Engin R*, 2003, 40: 47–102
  - 26 Marianetti C A. Electronic correlations in Li<sub>x</sub>CoO<sub>2</sub>. Doctor Dissertation. Cambridge: Massachusetts Institute of Technology, 2004. 51–83
  - 27 Van der Ven A. First principles investigation of the thermodynamic and kinetic properties of lithium transition metal oxides. Doctor Dissertation. Cambridge: Massachusetts Institute of Technology, 2000. 46–76
  - 28 Levi M D, Aurbach D. Frumkin intercalation isotherm—A tool for the description of lithium insertion into host materials: a review. *Electrochimica Acta*, 1999, 45: 167–185

## Science in China Series B: Chemistry

### EDITOR

XU Guangxian (Hsu, Kwang-Hsien)  
College of Chemistry and Molecular Engineering  
Peking University  
Beijing 100871, China

### AIMS AND SCOPE

*Science in China Series B: Chemistry*, an academic journal cosponsored by the Chinese Academy of Sciences and the National Natural Science Foundation of China, and published by Science in China Press and Springer, is committed to publishing high-quality, original results in both basic and applied research.

*Science in China Series B: Chemistry* is published bimonthly in both print and electronic forms. It is indexed by Science Citation Index.

**SUBMISSION: [www.scichina.com](http://www.scichina.com)**

### Orders and inquiries:

#### China

Science in China Press; 16 Donghuangchenggen North Street, Beijing 100717, China; Tel: +86 10 64034559 or +86 10 64034134; Fax: +86 10 64016350

#### North and South America

Springer New York, Inc.; Journal Fulfillment, P.O. Box 2485; Secaucus, NJ 07096 USA; Tel: 1-800-SPRINGER or 1-201-348-4033; Fax: 1-201-348-4505; Email: [journals-ny@springer-sbm.com](mailto:journals-ny@springer-sbm.com)

#### Outside North and South America

Springer Distribution Center; Customer Service Journals; Haberstr. 7, 69126 Heidelberg, Germany; Tel: +49-6221-345-0, Fax: +49-6221-345-4229; Email: [SDC-journals@springer-sbm.com](mailto:SDC-journals@springer-sbm.com)